Available online at www.sciencedirect.com
ScienceDirect
C. R. Physique 10 (2009) 504–513
COMPTES RENDUS PHYSIQUE
http://france.elsevier.com/direct/COMREN/

Theoretical spectroscopy / Spectroscopie théorique

Excitons in organic semiconductors

Peter Puschnig *, Claudia Ambrosch-Draxl

Chair of Atomistic Modelling and Design of Materials, Montanuniversität Leoben, Franz-Josef-Straße 18, A-8700 Leoben, Austria

Available online 5 December 2008

Abstract

In this article, excitonic effects in organic semiconductors investigated within the framework of many-body perturbation theory are reviewed. As an example for this technologically relevant class of materials the oligoacene series is studied. The electron–hole interaction is included by solving the Bethe–Salpeter equation for the electron–hole Green's function. This approach allows for the evaluation of the exciton binding energies, which are of major interest concerning the application in organic opto-electronic devices. We start the discussion with a comparison of the Kohn–Sham band structure with recent angular resolved photo-emission data. Starting from this one-electron band structure we focus on the impact of the electron–hole interactions on the optical properties by solving the Bethe–Salpeter equation. We demonstrate the dependence of the exciton binding energy on the molecular size and emphasize the effect of the intermolecular interaction on the exciton binding energies by means of pressure investigations. ***To cite this article: P. Puschnig, C. Ambrosch-Draxl, C. R. Physique 10 (2009).***

Résumé

Excitons dans des semiconducteurs organiques. Cet article passe en revue les effets excitoniques dans les semiconducteurs organiques dans le cadre de la théorie des perturbations à N particules. À titre d'exemple de cette classe de matériaux technologiquement importants, nous étudions la série des oligoacènes. L'interaction électronique est prise en compte en résolvant l'équation de Bethe–Salpeter pour la fonction de Green électron–trou. Cette approche permet l'évaluation des énergies de liaison électron-trou, qui sont d'importance majeure pour les applications aux dispositifs opto-électroniques. Nous commençons la discussion en comparant la structure de bande de Kohn–Sham avec des résultats récents de photoémission résolue en angle. En partant de la structure de bande à un électron, nous détaillons l'impact des interactions électron–trou sur les propriétés optiques en résolvant l'équation de Bethe–Salpeter. Nous démontrons que l'énergie de liaison de l'exciton dépend de la taille de la molécule et nous soulignons l'effet de l'interaction intermoléculaire sur les énergies de liaison excitoniques en nous appuyant sur des études en pression. ***Pour citer cet article : P. Puschnig, C. Ambrosch-Draxl, C. R. Physique 10 (2009).***

Keywords: Exciton; Organic semiconductor; Bethe–Salpeter equation

Mots-clés : Excitons ; Semiconducteur organique ; Équation Bethe–Salpeter

* Corresponding author.
E-mail addresses: peter.puschnig@mu-leoben.at (P. Puschnig), cad@mu-leoben.at (C. Ambrosch-Draxl).

1631-0705/$ – see front matter
doi:10.1016/j.crhy.2008.08.003

1. Introduction

In organic semiconductor research a huge variety of conjugated homo-, block-, and co-polymers have been synthesized and investigated in terms of their suitability to operate as active materials in devices such as organic light emitting diodes (OLEDs) [1–3], thin-film transistors (OTFTs) [4], photo-voltaic diodes (OPVDs) [5–7], or lasers [8,9]. In particular, polyacetylene (PA), poly(*p*-phenylene) (PPP), poly(*p*-phenylene vinylene) (PPV), polythiophene (PT), and polyfluorene (PF) backbones [10,11] have become prominent candidates for these applications. More recently, organic materials consisting of small π-conjugated molecules, which form well defined molecular crystals, have also attracted great attention; e.g., an OLED has been realized with *p*-sexiphenyl [12], which exhibits remarkable optical properties. The polarization of its electro-luminescence can be changed through the molecular alignment. Other examples are α-sexithiophene and pentacene, which have been successfully used in OTFTs [13–17].

In order to exploit the extraordinary electro-optical properties of these organic semiconductors and to tune them towards the requirements of interesting applications a detailed understanding of the fundamental physics is a prerequisite. While there has been a vast number of experimental investigations on their electronic and optical properties, both, for molecules in solution and in the bulk [18], theoretical models have been restricted to the treatment of isolated molecules. This is because, for a long time quantum chemical computations have been the method of choice, since these wave-function based schemes derived from the Hartree–Fock approach have proven to accurately characterize ground state as well as excited state geometries and transition energies for isolated molecules. Also calculations within density functional theory (DFT) have been very successful in describing equilibrium geometries of isolated molecules as well as excited state properties. Also the deficiency of standard exchange-correlation functionals when describing long-range interactions in one-dimensional systems has been investigated [19,20]. While there have also been attempts to tackle *intermolecular interactions* naturally arising in the bulk or in thin films within these quantum chemical cluster approaches [21–25], their unfavorable scaling did not allow for a comprehensive treatment of the full three-dimensional (3D) structure of real materials. In contrast, within density functional theory (DFT) the crystal periodicity of the organic semiconductors can be easily taken into account. Indeed, the importance of intermolecular interactions on the electronic and optical properties has been proven for several materials including oligoacenes [26–29], oligophenylenes [30–32], and PPV [33]. This also demonstrates that common exchange correlation functionals, such as the local density approximation (LDA) or the generalized gradient approximation (GGA), give a good description of the band structure of molecular crystals including intermolecular interactions. In particular, band dispersions and splittings found in the oligoacenes, for instance, are in good agreement with experimental findings [26,27,34,29]. For *bonding* properties, on the other hand, LDA commonly overestimates cohesive energies and underestimates intermolecular distances, while GGA gives hardly any binding. This deficiency can be traced back to missing van der Waals interactions which require a fully non-local correlation functional [35–37]. This issue is, however, outside the scope of the current review and can be safely ignored when working with molecular crystal structures based on experimental lattice constants.

DFT is strictly only applicable to the ground state, while an *ab-initio* description of *excited* states poses a much harder challenge. Here, many-body perturbation theory, in which the linear response is expressed in terms of the equation of motion for the electron–hole (e-h) two-particle Green's function, provides an adequate theoretical framework [38–44]. In the Bethe–Salpeter equation (BSE), the interaction between the electron and the hole is accounted for by an effective interaction kernel. To zeroth order, when the electron and hole are regarded as *independent* particles this results in the random phase approximation (RPA) for the optical properties. However, solutions of the BSE in an *ab-initio* framework, appearing in the literature in the past few years, have shown that e-h interactions are indeed important in order to correctly account for quantitative (oscillator strengths) as well as qualitative (bound excitons) features of optical spectra of semiconductors and insulators. This is true for inorganic [45–51] as well as for organic semiconductors [27,52–60]. The focus of the present article is on *excitonic* effects in *organic* semiconductors. Here, the exciton binding energy (BE) is a central quantity in the photophysics of these materials since it is intimately related to the probability of radiative emission/absorption and electric-field induced generation of free charge carriers. It is defined as the energy required to separate a bound e-h pair, the exciton, into a free electron and a free hole. We note that experimentally observed exciton BEs reported for PPV, for instance, range from 0.1 to 0.9 eV [61,62] thus giving controversial answers to the problem. Thus, the theoretical work reviewed herein contributed and helped to solve the debate whether the lowest energy transition is due to weakly bound Wannier excitons (or even independent charge carriers) or due to the absorption of tightly bound excitons (Frenkel exciton model) [63,23].

The remainder of the paper is organized as follows: Section 2 reviews the Bethe–Salpeter approach. Section 3 presents the crystal structures of the oligoacenes which we have chosen as representative samples for organic molecular crystals consisting of short π-conjugated oligomers. Before we review the optical properties of the oligoacenes, Section 4 compares the one-electron band structure resulting from the Kohn–Sham approach to recent photo-emission data. In the main part of the paper, Section 5, excitonic effects on the optical absorption properties of the oligoacenes, i.e. naphthalene (2A), anthracene (3A), tetracene (4A), and pentacene (5A) are reviewed. The systematic dependence on the molecular length, as well as the pressure dependence of the exciton binding energies is emphasized. The latter clearly demonstrates the importance of intermolecular interactions for the correct description of the optical properties. Finally, we will give a conclusion and an outlook.

2. Theoretical framework

Excited states can be rigorously described within many-body perturbation theory, which reduces the many-particle problem to an effective few-particle problem. All many-body effects are included in an effective interaction kernel, where the calculation of optical properties requires the knowledge of *two*-particle excitations. The equation of motion for the two-particle correlation function, the Bethe–Salpeter equation (BSE), accounts for the interaction between the electron and the hole in terms of an effective interaction kernel. Thus, the solution of the BSE represents a systematic first-principles approach for the calculation of optical absorption spectra including excitonic effects [64]. It is able to account for both, bound exciton states below the single-particle band gap, as well as for resonant excitons states above the band gap resulting in a redistribution of oscillator strengths compared to an independent e-h picture. The BSE can be expressed as a matrix eigenvalue equation [45,46,65]

$$\sum_{v'c'\mathbf{k}'} H^{e\text{-}h}_{vc\mathbf{k},v'c'\mathbf{k}'} A^{\lambda}_{v'c'\mathbf{k}'} = E^{\lambda} A^{\lambda}_{vc\mathbf{k}} \tag{1}$$

Here, $H^{e\text{-}h}$ is the effective electron–hole (e-h) Hamiltonian, the eigenvalues E^{λ} are the excitation energies, and the eigenvectors A^{λ} are the e-h coupling coefficients. The indices $vc\mathbf{k}$ denote a conduction (c) and valence (v) band of an electron and hole, respectively, corresponding to the Bloch vector $\mathbf{k}$. The e-h kernel $H^{e\text{-}h}$ is the sum of the repulsive exchange interaction H^{x}, the attractive direct, screened interaction H^{dir}, and the kinetic term H^{diag}. Thus the Hamiltonian consists of three parts

$$H^{e\text{-}h} = H^{\mathrm{diag}} + H^{\mathrm{dir}} + 2H^{x} \tag{2}$$

Note that the exchange term H^{x} is not active for spin *triplet* states, and the factor of 2 accounts for the spin degrees of freedom in spin *singlet* excitations. The expressions in Eq. (2) are given by the following relations [65]:

$$H^{\mathrm{diag}}_{vc\mathbf{k},v'c'\mathbf{k}'} = (E_{c\mathbf{k}} - E_{v\mathbf{k}})\delta_{vv'}\delta_{cc'}\delta_{\mathbf{k}\mathbf{k}'} \tag{3}$$

$$H^{\mathrm{dir}}_{vc\mathbf{k},v'c'\mathbf{k}'} = -\int \mathrm{d}^3r\,\mathrm{d}^3r'\,\psi_{v\mathbf{k}}(\mathbf{r})\psi^{*}_{c\mathbf{k}}(\mathbf{r}')W(\mathbf{r},\mathbf{r}')\psi^{*}_{v'\mathbf{k}'}(\mathbf{r})\psi_{c'\mathbf{k}'}(\mathbf{r}') \tag{4}$$

$$H^{x}_{vc\mathbf{k},v'c'\mathbf{k}'} = \int \mathrm{d}^3r\,\mathrm{d}^3r'\,\psi_{v\mathbf{k}}(\mathbf{r})\psi^{*}_{c\mathbf{k}}(\mathbf{r})\bar{v}(\mathbf{r},\mathbf{r}')\psi^{*}_{v'\mathbf{k}'}(\mathbf{r}')\psi_{c'\mathbf{k}'}(\mathbf{r}') \tag{5}$$

The first term, H^{diag}, only appears in the diagonal of the Hamilton matrix and contains energy differences between conduction and valence quasi-particle states. The direct interaction term H^{dir} is responsible for the attractive nature of the e-h interaction and hence for the formation of bound excitons. On the other hand, the exchange term H^{x} controls details of the excitation spectrum, such as the splitting between spin-singlet and spin-triplet excitations. Note that H^{dir} involves the *screened* Coulomb interaction

$$W = \epsilon^{-1}v \tag{6}$$

constructed from the inverse of the independent particle response ϵ and the bare Coulomb potential v. In contrast, H^{x} only contains the short-range part of the *bare* Coulomb interaction $\bar{v}$ [66,40].

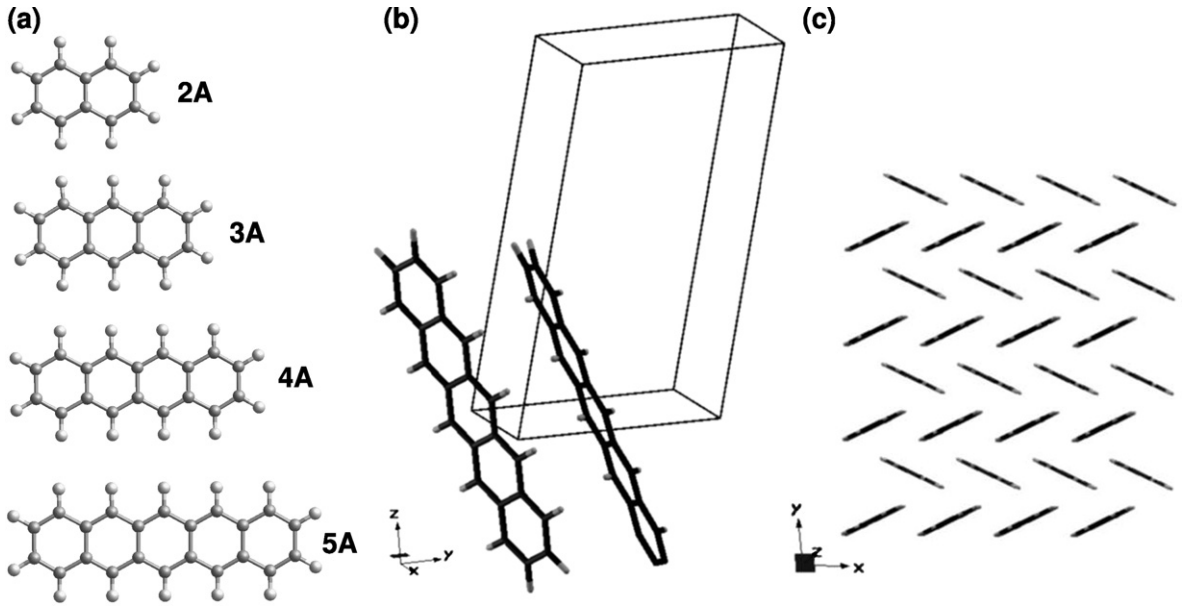

Fig. 1. (a) Chemical structure of the oligoacene molecules napthalene (2A), anthracene (3A), tetracene (4A), and pentacene (5A), respectively. (b) Crystal structure of pentacene showing the two inequivalent pentacene molecules per unit cell. (c) Top view of one layer of pentacene molecules exhibiting the characteristic herring-bone pattern.

3. Crystal structures

Oligoacene molecular crystals which are reviewed in the present work contain as basic building blocks aromatic phenyl rings. We study the series of the linear oligoacenes starting from napthalene (2A), anthracene (3A), tetracene (4A), and pentacene (5A) as depicted in the left part of Fig. 1. Due to the aromatic type of bonding the ring structures are rather rigid and can be considered to be completely planar. This planarity of the isolated molecules is also preserved in the crystal environment. Organic molecular crystals built by such rigid rod-like molecules typically exhibit low-symmetry crystal structures such as monoclinic and triclinic ones. The unit cell of the technologically most relevant representative, pentacene, is shown in the middle panel of Fig. 1. One repeat unit contains two inequivalent pentacene molecules. The center of mass of the first one is located at the origin of the cell, while the second one is positioned in the middle of the *ab* plane. The long molecular axis of both molecules are aligned almost parallel while the molecular plane normals enclose a characteristic angle. This arrangement gives rise to a structural feature, which is characteristic of many molecular crystals consisting of rigid rod-like building blocks, which is the formation of a so-called *herringbone* pattern in the *ab* plane. This can be seen in Fig. 1c which shows a projection of the crystal structure perpendicular to the long molecular axis. The herringbone stacking is the result of a compromise between steric hindrance and orbital overlap in such systems [28,31,30]. Along the *c* direction the crystal structure is characterized by layers comprised of almost upright standing molecules, i.e., the thickness of these layers approximately corresponds to the length of one molecule.

For the calculations presented herein we have taken experimental values for the lattice constants measured at ambient conditions [67–70]. For the investigation of the pressure dependence on the exciton binding energy which gives insight into the role of intermolecular interactions, we use the pressure dependent lattice parameters of anthracene published elsewhere [71]. If hydrostatic pressure is applied, the intermolecular distances are reduced resulting in an enhancement of the intermolecular interactions, which is accompanied by an increase of the herringbone angle. Thus, the application of pressure provides the possibility to investigate the sensitivity of the exciton binding energies on changes in the intermolecular bonding.

4. One-particle band structure

A prerequisite for the treatment of optical properties within the framework of many-body perturbation theory is the knowledge of the one-electron quasi-particle band structure and wave functions. Thus, within this section we

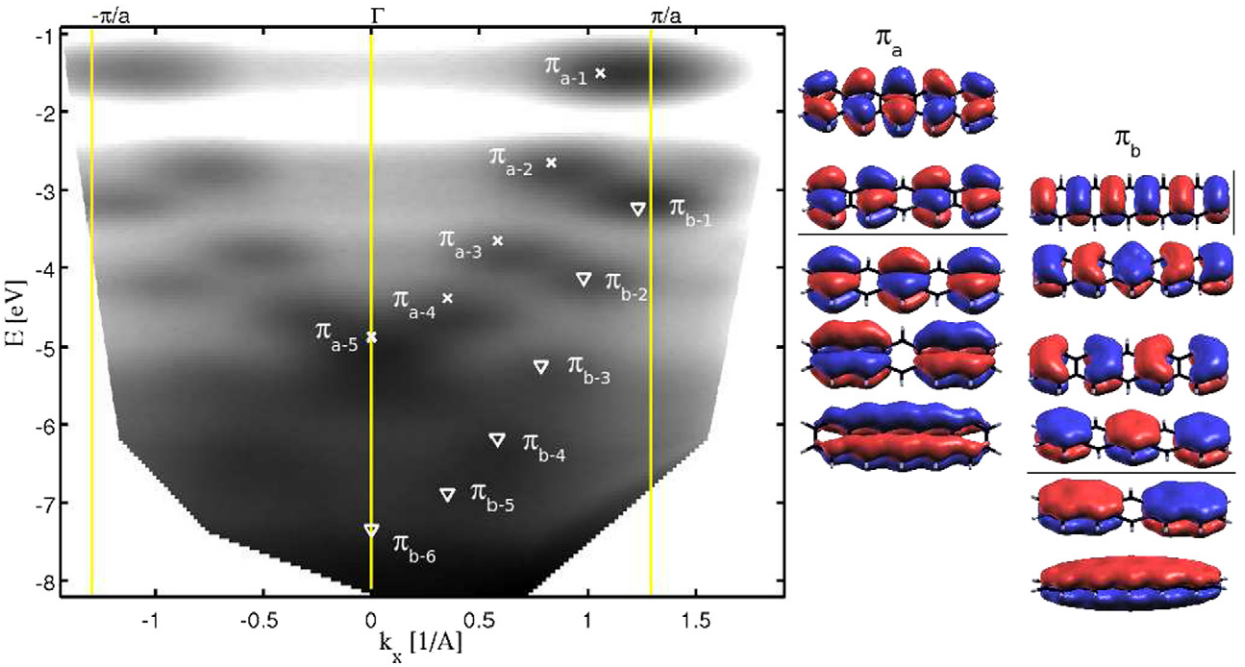

Fig. 2. Left panel: Angular resolved photo-emission data of a pentacene thin film displayed as a density map, electron binding energy versus momentum parallel to the long molecular axis [29]. The symbols indicate the energy and momentum position from isolated molecule calculations as explained in the text. The right part of the figure displays the corresponding molecular orbitals of the two occupied π bands.

discuss the electronic band structure for the most important representative of the linear oligoacene family, i.e., the five-ring oligoacene, pentacene (5A). We approximate the quasi-particle band structure and wave functions by the corresponding Kohn–Sham band structure and orbitals obtained within the framework of density functional theory. A comparison of the so-obtained valence band structure of pentacene with recent photo-emission data is given in Fig. 2. There, angular resolved photo-emission from an ordered film of pentacene in a plane *parallel* to the long molecular axis [29] (density map) is compared to Kohn–Sham energies (symbols). Given the π-conjugated nature of the pentacene molecule, the highest occupied molecular orbitals as well as the lowest unoccupied ones (not shown) exhibit π symmetry. Since each of the 22 carbon atoms contributes one p_z-orbital, there will be 11 fully occupied π orbitals which give rise to two molecular bands: five orbitals from the pairs of apex carbons with nodal planes perpendicular to the molecular plane, and six from the linking and end carbon pairs. The Kohn–Sham orbitals of these states are depicted in the right panel of Fig. 2.

It is clear that molecular orbitals of a single molecule cannot strictly be ascribed to a definite wave vector k. Nevertheless, the behavior of the orbitals can be interpreted in terms of an *intra*molecular band structure. In this finite five-ring system, however, the limited number of units leads to discrete orbitals, rather than a continuous band. As a consequence, we observe the momentum of each orbitals to be spread in reciprocal space where the width is proportional to the inverse length of the molecule. States derived from an infinite chain would, in contrary, be infinitely sharp in momentum space. The symbols in Fig. 2 overlayed the experimental photo-emission band map are in fact the outcome of a DFT calculation for an isolated 5A molecule. The position on the momentum axis indicates the peak of the Fourier transform of the respective Kohn–Sham orbital in the direction parallel to the long molecular axis. Simply speaking, the position in k space it is related to the inverse distance of two adjacent nodal planes in the wave function. Thus, the k vector increases from bottom to top leading to two parabola-like *intra*molecular bands. The reason why such a behavior is indeed observed in photo-emission can be understood in terms of the photo-emission transition matrix elements. These are proportional to the Fourier transform of the initial state wave function if the final state is approximated by a simple plane wave [72,32,29]. Note that the Kohn–Sham eigenvalues are shifted such that the energy of the highest occupied molecular orbital (HOMO) matches the experimental value. The excellent agreement between experiment and theory demonstrates that the Kohn–Sham energies and orbitals serve as a reliable starting point for the treatment of optical properties within the BSE approach.

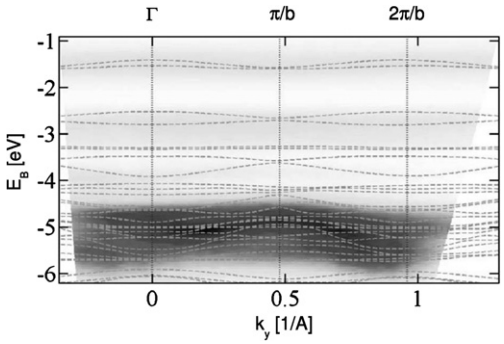

Fig. 3. Angular resolved photoemission data perpendicular to the 5A molecular axes [29]. The Brillouin zone boundaries of the 5A crystal along the crystal b axis are indicated. The gray scale represents an arbitrary intensity scale. The DFT band structure is shown by the dashed lines.

To a large extent the electronic structure of molecular crystals can be understood in terms of the electronic structure of their molecular building blocks. As demonstrated above, the band structure parallel to the long molecular axis can be accounted for by the *intra*molecular dispersion of individual molecules. This is because the *inter*molecular interaction in this direction is very small as can be seen from the crystal structure depicted in Fig. 1. For directions perpendicular to the long molecular axis, i.e., parallel to the herring bone layer, on the other hand, there is considerable intermolecular interaction leading to sizeable band dispersion in the order of 0.5 eV. This can be seen from Fig. 3 where the band map measured from angular resolved photo-emission is compared to a DFT band structure along the crystal *b* axis, i.e., perpendicular to the long molecular axis. The experimentally observed continuous bands are in agreement with the Kohn–Sham bands calculated for bulk 5A. For instance, the dispersion of the HOMO is in accord with theory, both in magnitude and direction [29].

We conclude this section about the one-particle band structure by stating that Kohn–Sham energies and orbitals of oligoacene molecular crystals serve as a reliable starting point for the treatment of electron–hole interactions within the framework of the Bethe–Salpeter equation. This has been demonstrated above for the *occupied* bands by comparison with angular resolved photo-emission spectra. We emphasize the well-known fact that density functional theory systematically underestimates band gaps of semi-conductors and insulators. Within this work we do not attempt to correct for this shortcoming by calculating the quasi-particle band structure within the GW approximation. However, a comparison of the GW band structure of pentacene with the corresponding GGA one has revealed that the bands energetically close to the band gap are well described by a scissors-shift of the GGA bands [27]. Therefore, we resort to a simple scissors shift for the *unoccupied* which serves to be an excellent approximation in this class of materials.

5. Excitonic effects in optical properties

Exciton binding energies (BE) are of major interest concerning the application in organic opto-electronic devices. For instance, in photo-voltaic devices an effective charge separation is only achieved, if the electron and hole can easily be moved apart from each other. On the other hand, organic light emitting diodes exhibiting a high photoluminescence quantum yield require the electron–hole pair to be spatially confined, i.e., a high exciton BE. We demonstrate below that within the family of molecules investigated here both limiting scenarios can be achieved. The exciton binding energy is obtained by solving the Bethe–Salpeter equation and comparing the resulting optical spectra with the independent electron–hole result obtained within the RPA. We focus on two interesting questions, namely: (i) how the exciton BE depends on the molecular length; and (ii) how the intermolecular interactions influence the strength of the electron–hole correlations.

5.1. Dependence on molecular length

Here we investigate how the exciton binding energy depends on the length of the molecular building blocks. We review the findings for the series of oligoacenes from naphthalene (2A) to pentacene (5A). Fig. 4 compares the RPA spectra (shaded areas) with the optical absorption spectra resulting from the Bethe–Salpeter approach for light polarized perpendicular to the long molecular axis. Thus, the arrows indicate the size of the exciton binding energy.

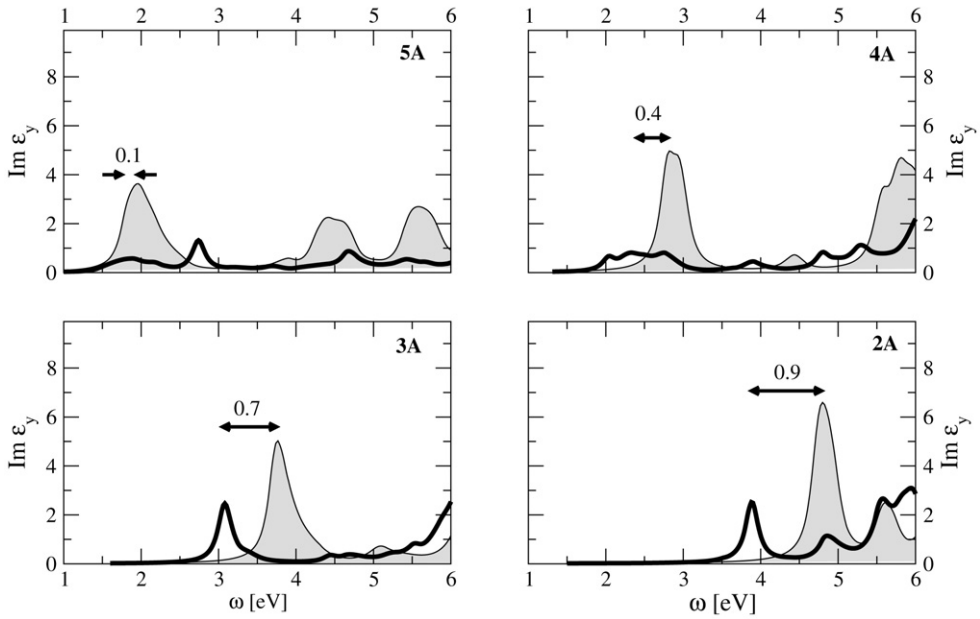

Fig. 4. The imaginary part of the dielectric function for the oligoacenes, 2A (bottom right), 3A (bottom left), 4A (top right), and 5A (top left), respectively. For comparison the RPA spectrum (shaded areas) as well as the BSE spectra including excitonic effects are shown and the exciton binding energies of the lowest singlet states are indicated.

Compared to experiment, the RPA peak positions greatly overestimate the transition energies due to the missing electron–hole interaction. On the other hand, the peak positions at 3.9 eV (2A), 3.1 eV (3A), 2.4 eV (4A), and 1.9 eV (5A) resulting from the BSE compare favorably with experimental values highlighting the importance of excitonic effects [58].

Turning the discussion to exciton binding energies, we find a significant reduction from 0.9 eV (2A) to 0.7 eV (3A), 0.4 eV (4A), and 0.1 eV (5A) as can be seen from Fig. 4. This trend is also observed experimentally with values ranging from 1.0–1.5 eV for 2A, 0.4–1.1 eV for 3A, 0.1–1.0 eV for 4A, and 0.0–0.5 eV for 5A, respectively [18,73]. The reduction of the exciton binding energy with increasing molecular length is a common feature found also in the phenylenes as well as in the thiophenes [74]. It is a consequence of the decreasing e-h Coulomb interaction, when the molecular size increases, and can be attributed to two effects: (i) a larger extension of the e-h wave function; and (ii) the strong enhancement of the dielectric screening. While the latter is a result of the reduction of the electronic band gap with increasing molecular length, the former can be explained by spatially more extended electron clouds along the molecular backbone allowing for a larger separation of the electron and the hole, when the length of the molecule increases.

5.2. Role of intermolecular interactions

The optical properties of *isolated* oligoacene molecules have been the subject of intense theoretical research where methods ranging from time-dependent density functional theory (TDDFT) to wave function based approaches, i.e., configuration interaction (CI) schemes, have been applied [75]. When measurements for acenes in solution are corrected for solvent effects one finds good agreement between theory and experiment. For the lowest energy transition polarized parallel to the short molecular axis TDDFT results are reported to lie somewhat below the experimental data where the error increases with the length of the molecule, while CI overestimates experimental excitation energies [75]. When comparing measurements in solution to data taken from thin films one notices a red-shift of the first absorption peak [58,75]. This can be attributed to intermolecular interactions.

The application of external hydrostatic pressure varies the intermolecular distances in a very defined way allowing for a precise analysis of the influence of intermolecular interactions on the excitonic properties. In agreement with experimental X-ray data, calculations of the structural properties of the oligophenylenes [31] and anthracene [28] have

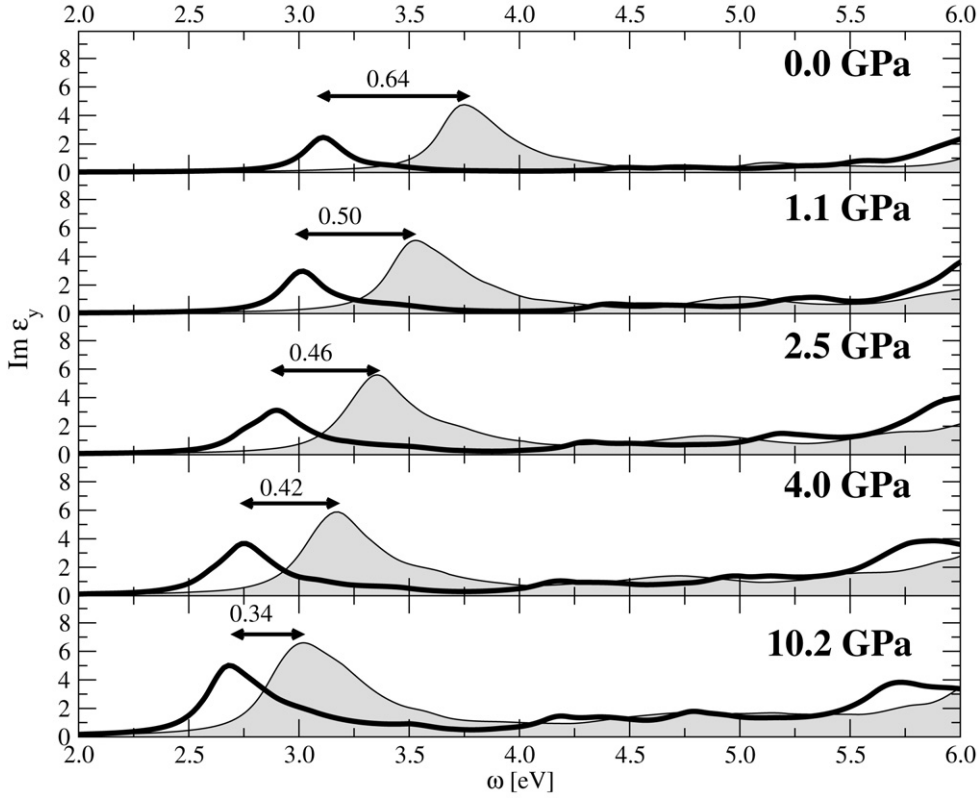

Fig. 5. The imaginary part of the dielectric function for the anthracene as a function of applied pressures for 0.0, 1.1, 2.5, 4.0 and 10.2 GPa, respectively (from top to bottom). For comparison the RPA spectrum (shaded areas) as well as the BSE spectra including excitonic effects are shown and the exciton binding energies of the lowest singlet states are indicated.

indeed shown that the main structural changes under pressure are a reduction of the intermolecular distances and a modification in the molecular conformation (herringbone angle), whereas the internal geometry of the molecules (bond lengths and angles) is only slightly affected. This is a result of the rather weak intermolecular forces as compared to the strong covalent intramolecular bonds. Therefore, pressure proves to be a suitable way to study the dependence of excitonic properties on intermolecular interactions. Starting from the pressure dependent crystal structures, exciton binding energies as a function of pressure are obtained by applying the BSE approach.

From the arguments outlined above it can already be anticipated that the exciton binding energy reduces, when hydrostatic pressure is applied. This is indeed observed for anthracene (Fig. 5) and has also been found for 2P [76]. The BE of anthracene decreases with pressure from 0.66 eV at ambient pressure to 0.34 eV at 10.2 GPa. Similar trends are also observed for 2P where the reduction in the BE lies between 0.70 and 0.55 eV, when going from ambient pressure to 5 GPa. As has been demonstrated for anthracene, the reduction in the BE is a consequence of the increased intermolecular interactions resulting in an enhanced wave function overlap and larger band dispersions. The increase in the spatial extent of the e-h function can also be explained from the respective e-h wave functions [55]. If pressure is applied, the extension of the singlet exciton in the herringbone *ab* plane is highly increased, whereas the e-h wave function remains rather confined in *c* direction. While the former is the reason for the significant reduction of SBE with pressure, the latter ensures that the electron and the hole are still bound.

6. Conclusions

In the present work we have reviewed the exciton binding energies in the oligoacene series which serve as prototypical examples for organic semiconductors based on short π-conjugated molecules. We adopt an ab-initio approach based on the Bethe–Salpeter equation for the electron–hole pair and focus on the size of the exciton binding energy. We study its dependence on the molecular size and discuss the effect of the intermolecular interactions by applying

external pressure. It turns out that organic molecular crystals built by short molecules give rise to exciton binding energies in the range of 0.8–0.9 eV. However, the they are significantly reduced when increasing the oligomer length. In the case of the series of oligoacenes, the electron–hole binding energy is very effectively reduced with increasing oligomer length, i.e., 0.9 eV in naphthalene, whereas in pentacene it amounts to only 0.1 eV.

As already mentioned above the magnitude of the exciton binding energy is important in terms of electro-optical applications. In photo-voltaic devices, for instance, an efficient operation requires the electron and hole to be easily separable. Thus, from our results we can conclude that dense molecular structures with sizeable intermolecular interactions should perform favorable. Also, the longer molecular building blocks support the goals of low exciton binding energies. On the other hand, organic light emitting diodes, where high photoluminescence quantum yields (high recombination rates) are desired, demand large exciton binding energies. The associated spatial confinement of the electron–hole pair can be achieved by using short molecules. These exhibit large band gaps which give rise and consequently lead to a weak dielectric screening of the electron–hole interaction. Equally important for that goal is to prevent intermolecular interactions, for instance, by choosing molecular building blocks with bulky side-groups. Thereby open structures are created which show little intermolecular wave-function overlap.

Acknowledgements

We acknowledge financial support from the Austrian Science Fund, FWF project P16227, and the EU RT network EXCITING, HPRN-CT-2002-00317. We are indebted to S. Berkebile and M. Ramsey for providing us with the experimental photo-emission data. Last but not least we greatly acknowledge K. Hummer who has published much of the original work on oligoacene exciton binding energies.

References

[1] C.W. Tang, S.A. VanSlyke, Appl. Phys. Lett. 51 (1987) 913.
[2] J.H. Burroughes, et al., Nature 347 (1990) 539.
[3] R. Friend, et al., Nature 397 (1999) 121.
[4] C.D. Dimitrakopoulos, D.J. Mascaro, IBM J. Res. & Dev. 45 (2001) 11.
[5] N.S. Sariciftci, L. Smilowitz, A.J. Heeger, F. Wudl, Science 258 (1992) 1474.
[6] M. Granström, et al., Nature 395 (1998) 257.
[7] C.J. Brabec, N.S. Sariciftci, J.C. Hummelen, Adv. Funct. Mater. 11 (2001) 15.
[8] R.C. Polson, Z.V. Vardeny, Phys. Rev. B 71 (2005) 45205.
[9] G. Strangi, et al., Phys. Rev. Lett. 94 (2005) 63903.
[10] D. Kim, H. Cho, C.Y. Kim, Prog. Polym. Sci. 25 (2000) 1089.
[11] A.J. Heeger, Synth. Met. 125 (2002) 23.
[12] M. Era, T. Tsutsui, S. Saito, Appl. Phys. Lett. 67 (1995) 2436.
[13] L. Torsi, A. Dodabalapur, L.J. Rothberg, A.W.P. Fung, H.E. Katz, Science 272 (1996) 1462.
[14] C.D. Dimitrakopoulos, A.R. Brown, A. Pomp, J. Appl. Phys. 80 (1996) 2501.
[15] S. Nelson, Y.-Y. Lin, D.J. Gundlach, T.N. Jackson, Appl. Phys. Lett. 72 (1998) 1854.
[16] G. Horowitz, Adv. Mater. 10 (1998) 365.
[17] L. Torsi, et al., Sol. State Electronics 45 (2001) 1479.
[18] M. Pope, C.E. Swenberg, Electronic Processes in Organic Crystals and Polymers, Oxford University Press, New York, 1999.
[19] K.N. Kudin, R. Car, R. Resta, J. Chem. Phys. 122 (2005) 134907.
[20] J.A. Berger, P.L. de Boeij, R. van Leeuwen, J. Chem. Phys. 123 (2005) 174910.
[21] J. Cornil, D. Beljonne, J.L. Brédas, J. Chem. Phys. 103 (1995) 834.
[22] J.L. Brédas, Synth. Met. 84 (1997) 3.
[23] Z. Shuai, D. Beljonne, R.J. Silbey, J.L. Brédas, Phys. Rev. Lett. 84 (2000) 131.
[24] J.L. Brédas, J.P. Calbert, D.A. da Silva Filho, J. Cornil, Proc. Nat. Acad. Sci. 99 (2002) 5804.
[25] Y.C. Cheng, et al., J. Chem. Phys. 118 (2003) 3764.
[26] R.G. Endres, C.Y. Fong, L.H. Yang, G. Witte, C. Wöll, Comp. Mat. Sci. 29 (2004) 362.
[27] M.L. Tiago, J.E. Northrup, S.G. Louie, Phys. Rev. B 67 (2003) 115212.
[28] K. Hummer, P. Puschnig, C. Ambrosch-Draxl, Phys. Rev. B 67 (2003) 184105.
[29] S. Berkebile, et al., Phys. Rev. B 77 (2008) 115312.
[30] G. Heimel, et al., J. Phys. Cond. Matt. 15 (2003) 3375.
[31] P. Puschnig, et al., Phys. Rev. B 67 (2003) 235321.
[32] G. Koller, et al., Science 317 (2007) 351.
[33] A. Ferretti, A. Ruini, E. Molinari, M.J. Caldas, Phys. Rev. Lett. 90 (2003) 86401.
[34] K. Hummer, C. Ambrosch-Draxl, Phys. Rev. B 72 (2005) 205205.

[35] M. Dion, H. Rydberg, E. Schroeder, D.C. Langreth, B.I. Lundqvist, Phys. Rev. Lett. 92 (2004) 246401.
[36] J. Kleis, B.I. Lundqvist, D.C. Langreth, E. Schröder, Phys. Rev. B 76 (2007) 100201(R).
[37] D. Nabok, P. Puschnig, C. Ambrosch-Draxl, Phys. Rev. B 77 (2008) 245316.
[38] L.J. Sham, T.M. Rice, Phys. Rev. 144 (1966) 708.
[39] W. Hanke, L.J. Sham, Phys. Rev. B 12 (1975) 4501.
[40] W. Hanke, Adv. Phys. 27 (1978) 287.
[41] W. Hanke, L.J. Sham, Phys. Rev. Lett. 43 (1979) 387.
[42] W. Hanke, L.J. Sham, Phys. Rev. B 21 (1980) 4656.
[43] G. Strinati, Phys. Rev. Lett. 49 (1982) 1519.
[44] G. Strinati, Phys. Rev. B 29 (1984) 5718.
[45] S. Albrecht, G. Onida, L. Reining, Phys. Rev. B 55 (1997) 10278.
[46] L.X. Benedict, E.L. Shirley, R.B. Bohn, Phys. Rev. Lett. 80 (1998) 4514.
[47] M. Rohlfing, S.G. Louie, Phys. Rev. Lett. 81 (1998) 2312.
[48] P. Puschnig, C. Ambrosch-Draxl, Phys. Rev. B 66 (2002) 165105.
[49] R. Laskowski, N.E. Christensen, G. Santi, C. Ambrosch-Draxl, Phys. Rev. B 72 (2005) 035204.
[50] S. Albrecht, L. Reining, R. Del Sole, G. Onida, Phys. Rev. Lett. 80 (1998) 4510.
[51] B. Arnaud, M. Alouani, Phys. Rev. B 63 (2001) 085208.
[52] M. Rohlfing, S.G. Louie, Phys. Rev. Lett. 82 (1999) 1959.
[53] G. Bussi, et al., Appl. Phys. Lett. 80 (2002) 4118.
[54] P. Puschnig, C. Ambrosch-Draxl, Phys. Rev. Lett. 89 (2002) 056405.
[55] K. Hummer, P. Puschnig, C. Ambrosch-Draxl, Phys. Rev. Lett. 92 (2004) 147402.
[56] M.L. Tiago, M. Rohlfing, S.G. Louie, Phys. Rev. B 70 (2004) 193204.
[57] E. Artacho, et al., Phys. Rev. Lett. 93 (2004) 116401.
[58] K. Hummer, C. Ambrosch-Draxl, Phys. Rev. B 71 (2005) 081202(R).
[59] A. Ruini, M.J. Caldas, G. Bussi, E. Molinari, Phys. Rev. Lett. 88 (2002) 206403.
[60] J.-W. van der Horst, P.A. Bobbert, M.A.J. Michels, G. Brocks, P.J. Kelly, Phys. Rev. Lett. 83 (1999) 4413.
[61] D. Moses, J. Wang, A.J. Heeger, N. Kirova, S. Brazovski, Synth. Met. 125 (2002) 93.
[62] S.V. Frolov, Z. Bao, M. Wohlgenannt, Z.B. Vardeny, Phys. Rev. Lett. 85 (2000) 2196.
[63] D. Moses, C. Soci, P. Miranda, A.J. Heeger, Chem. Phys. Lett. 350 (2001) 531.
[64] G. Onida, L. Reining, A. Rubio, Rev. Mod. Phys. 74 (2002) 601.
[65] M. Rohlfing, S.G. Louie, Phys. Rev. B 62 (2000) 4927.
[66] V. Ambegaokar, W. Kohn, Phys. Rev. 117 (1960) 423.
[67] D.W.J. Cruickshank, Acta Cryst. 10 (1957) 504.
[68] R. Mason, Acta Cryst. 17 (1964) 547.
[69] J.M. Robertson, V.C. Sinclair, J. Trotter, Acta Cryst. 14 (1961) 697.
[70] R.B. Campbell, J.M. Robertson, J. Trotter, Acta Cryst. 14 (1961) 705.
[71] M. Oehzelt, R. Resel, A. Nakayama, Phys. Rev. B 66 (2002) 174104.
[72] E.L. Shirley, L.J. Terminello, A. Santoni, F.J. Himpsel, Phys. Rev. B 51 (1995) 13614.
[73] E.A. Silinsh, Organic Molecular Crystals, Springer-Verlag, Berlin, 1980.
[74] K. Hummer, P. Puschnig, S. Sagmeister, C. Ambrosch-Draxl, Mod. Phys. Lett. B 20 (2006) 261.
[75] E.S. Kadantsev, M.J. Stott, A. Rubio, J. Chem. Phys. 124 (2006) 134901.
[76] C. Ambrosch-Draxl, K. Hummer, S. Sagmeister, P. Puschnig, Chem. Phys. 325 (2006) 3.